Neptune kick-off meeting
Catania 14/12/2018 WP 2

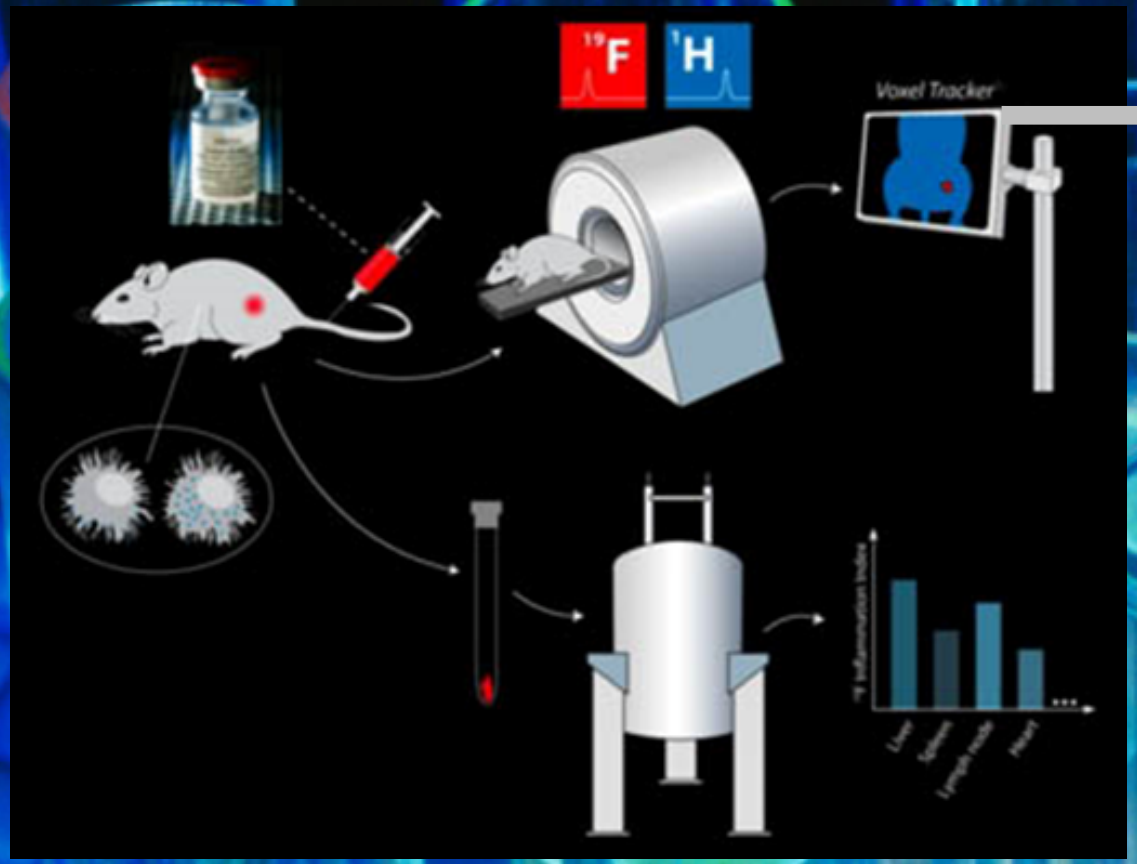

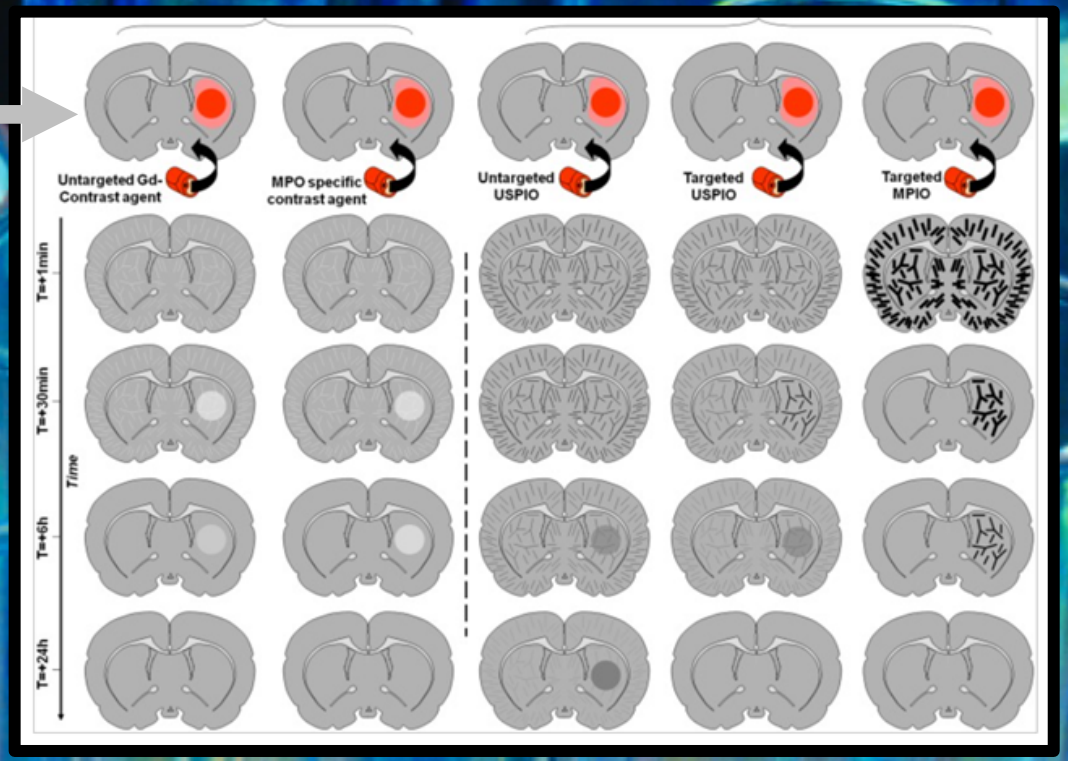

Drugs monitoring by 19F-MR imaging and 19F-MR spectroscopy

Silvia Capuani | CNR ISC | Physics Dpt. Sapienza University of Rome silvia.capuani@roma1.infn.it

Nuclear Magnetic Resonance Imaging (MRI)

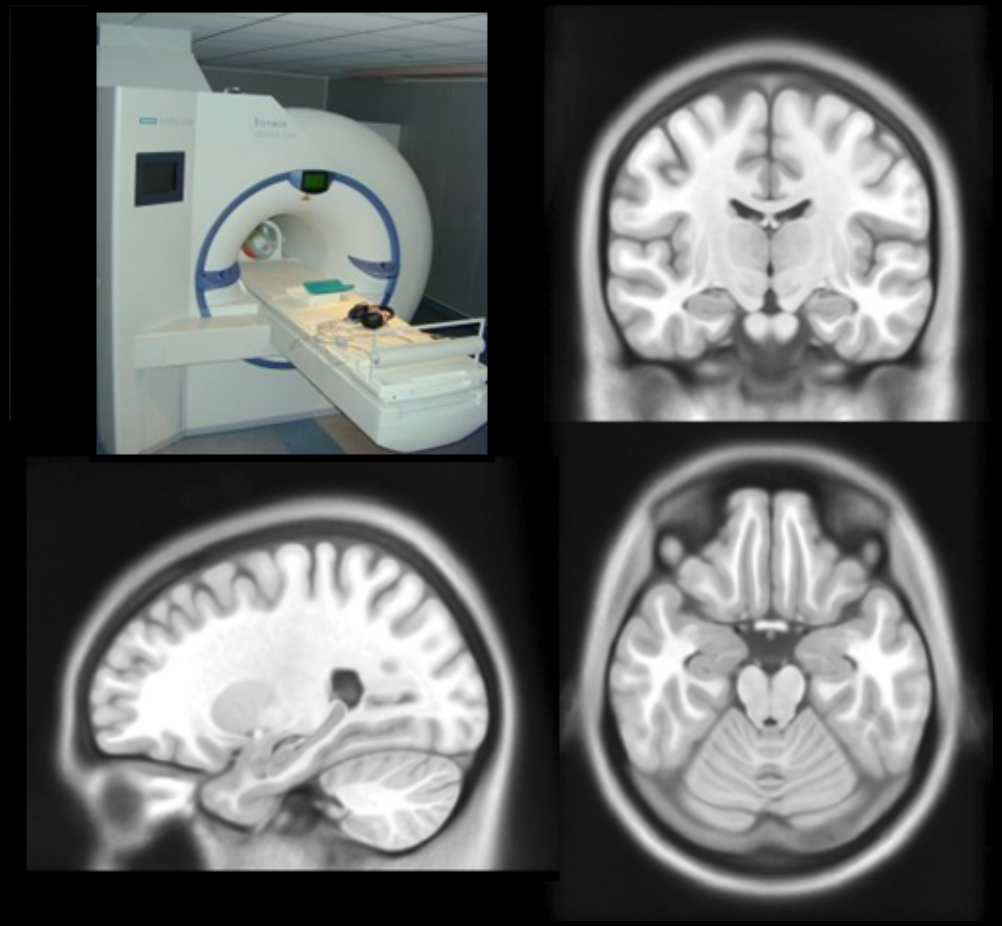

Signal from hydrogen nuclei

MRI scans essentially map the location of water and fat in the body

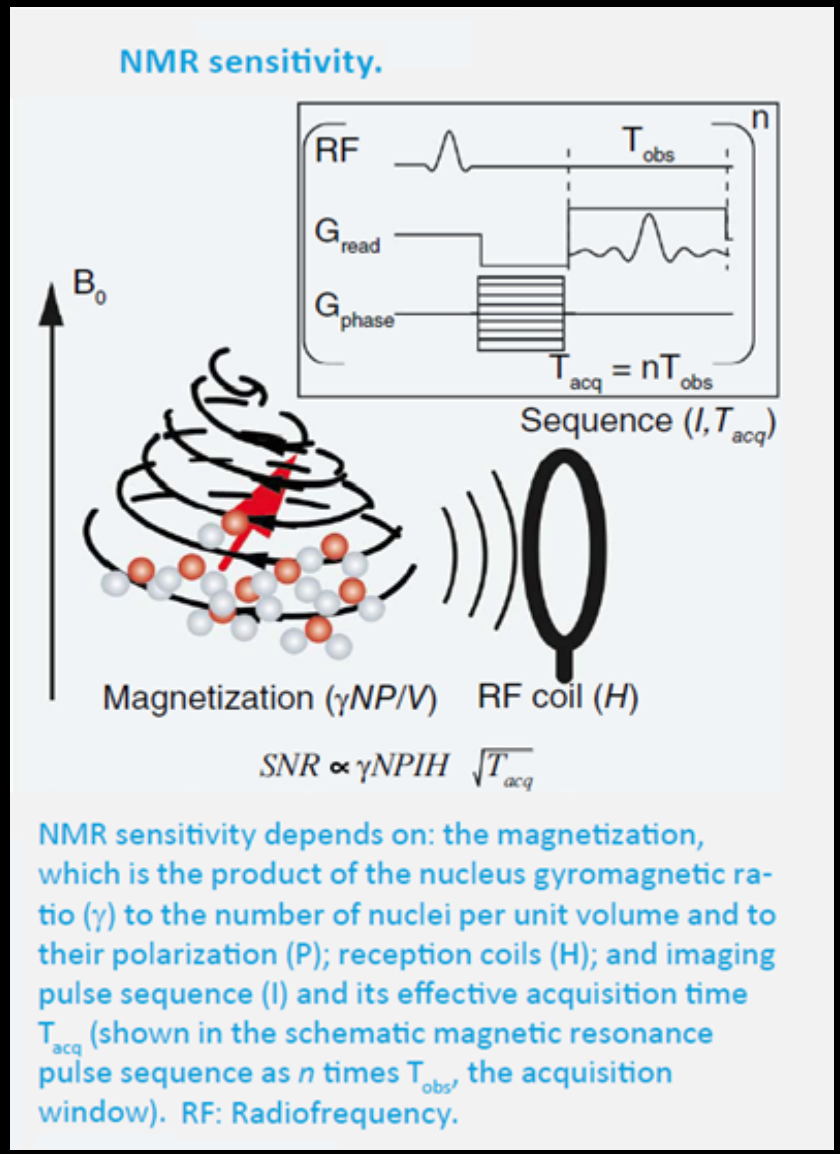

NMR sensitivity depends on: the magnetization, which is the product of the nucleus gyromagnetic ratio (γ) to the number of nuclei per unit volume and to their polarization (P); reception coils (H); and imaging pulse sequence (I) and its effective acquisition time T_{acq} (shown in the schematic magnetic resonance pulse sequence as *n* times T_{obs}, the acquisition window). RF: Radiofrequency.

Conventional magnetic resonance (MR) techniques are based on the detection of the signal from mobile protons (hydrogen 1[1H]) of water or lipids (concentration of protons 50 M). Protons are highly abundant in the body, and their concentration and magnetic properties (relaxations times T1, T2) vary with anatomy.

19F NMR

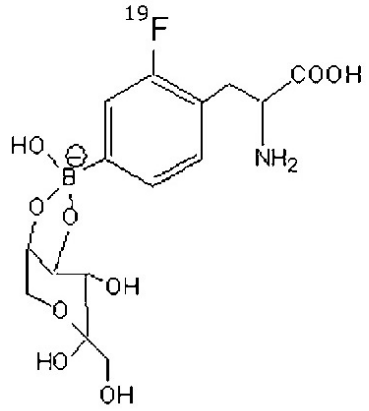

F-BPA fructose-complex

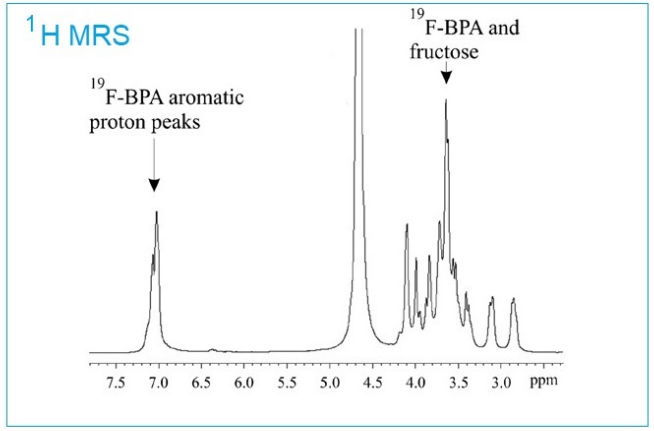

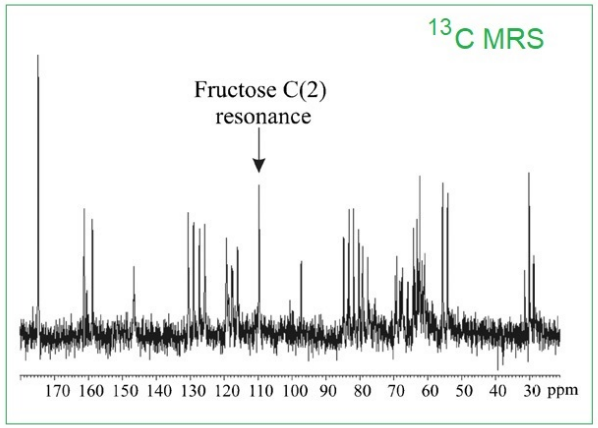

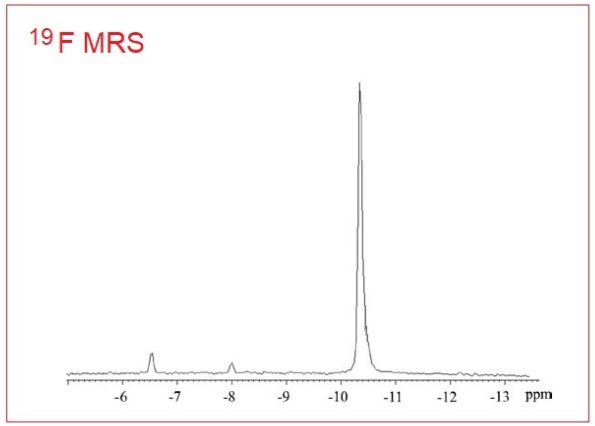

P. Porcari, S. Capuani et al. Phys Med Biol 2006

Due to the absence of NMR-visible 19F in living tissues, 19F MRI has the strong advantage over 1H MRI to specifically detect administered 19F-containing compounds without background signal, and to yield a linear relationship between signal and concentration of contrast agent. These properties, combined with the fact that 19F is the most sensitive nucleus after 1H, have raised much enthusiasm about 19F MRI emerging as a potential substitute to PET imaging

19F has 100% natural abundance,
spin = 1/2, and a gyromagnetic ratio slightly lower than that of of 1H, resulting in 83% of the sensitivity of 1H.

With seven outer-shell electrons, 19F chemical shifts (CSs) are more sensitive to the local environment than 1H with its single electron. Indeed, the spectroscopic signatures of 19F compounds can vary over a range more than 200 ppm, offering the potential for definitive identification of many compounds even at lower clinical field strengths

19F cells tracking by MRI and MRS

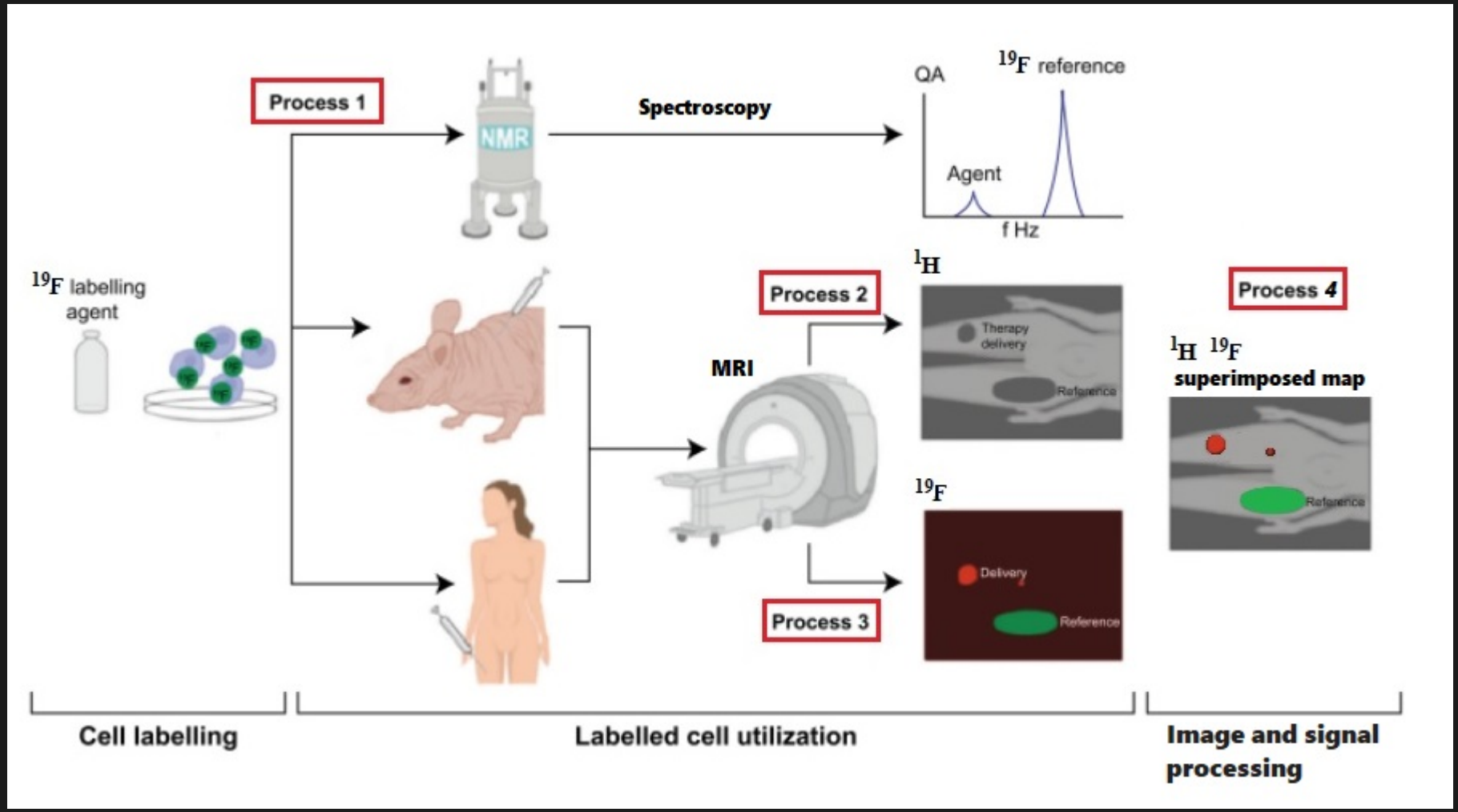

^{19}F-MRI and ^{19}F-MRS in C6 bearing rat brain

^{19}F-MRI and ^{19}F-MRS were used to obtain in vivo spatial distribution mapping and pharmacokinetic of BPA

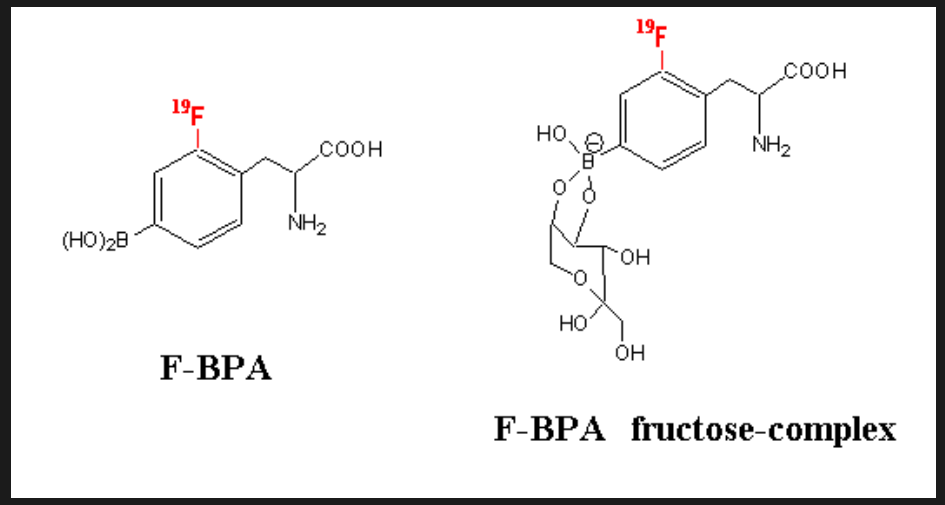

BNCT

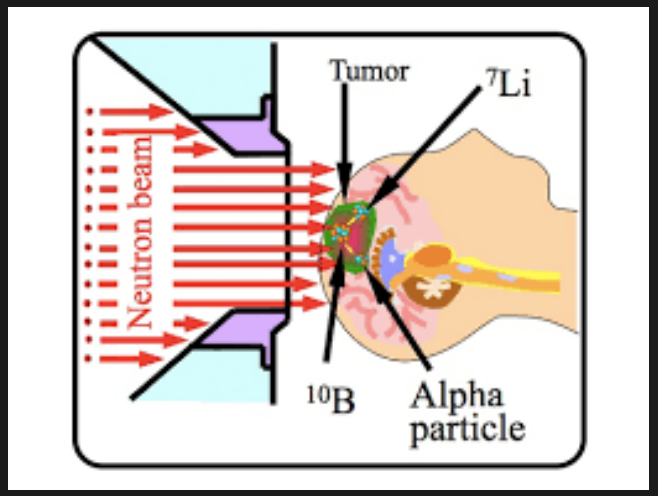

to investigate the use of L-DOPA as enhancer for BPA uptake in C6-glioma cells

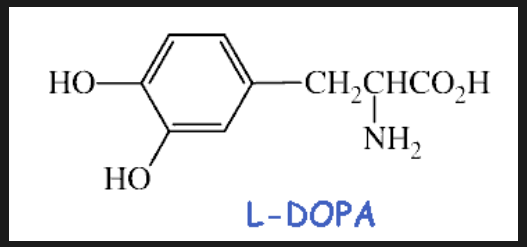

Animal model

Animal model: C6-glioma rat brain

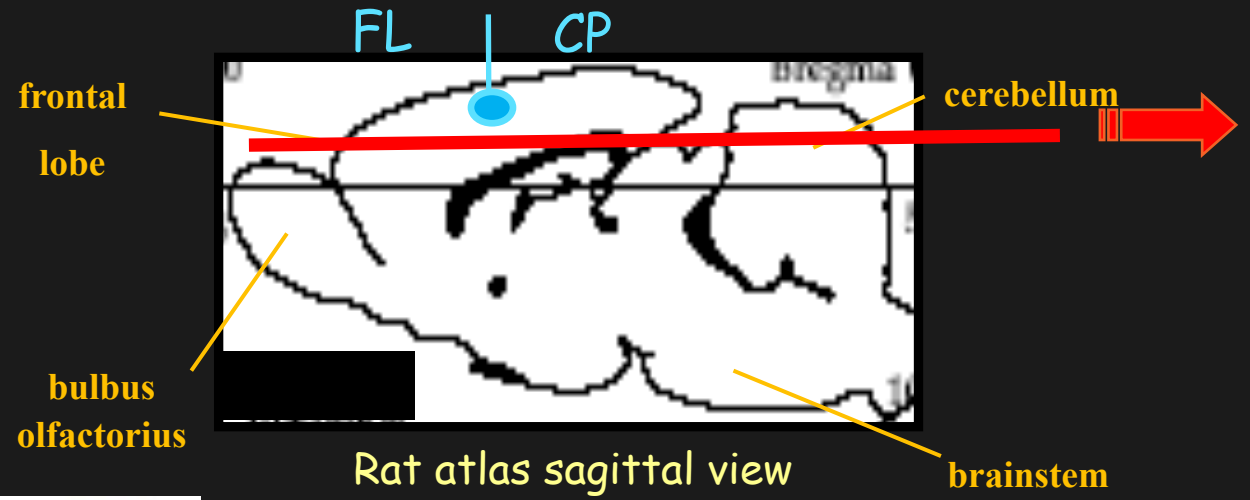

Rat atlas sagittal view

Anatomical ^{1}H images

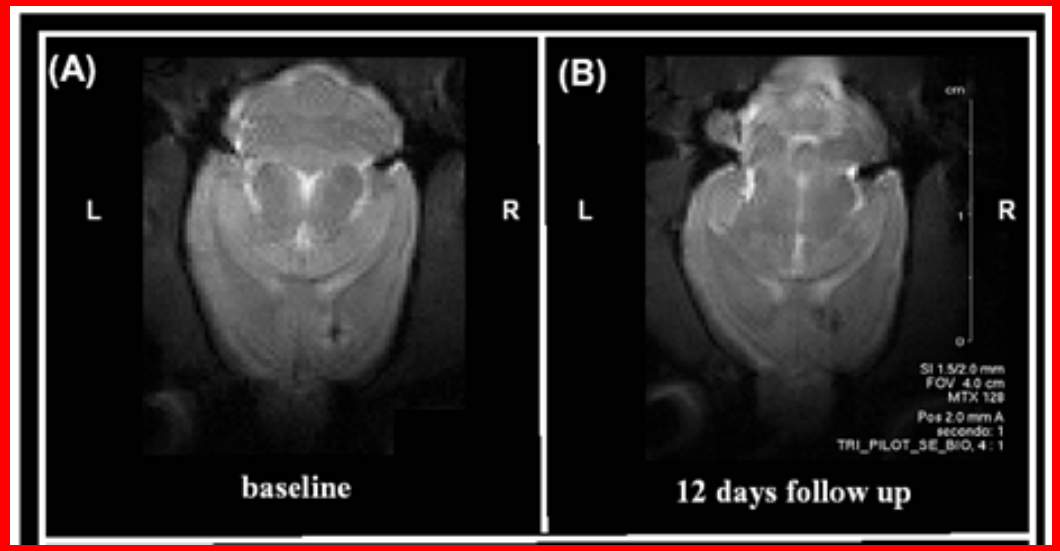

Axial view NMR images

25 Male Wistar rats (300-350g) were anesthetized by intraperitoneal injection of ketamine (60mg/kg) and xylazina before being fixed in a stereotactic frame. A middle scalp incision was made and C6 cell suspension (**10^6 cells in 10 µl**) was slowly injected with a Hamilton syringe through a burr hole in the right hemisphere, 3 and 4 mm depth from the *dura*. Then, the syringe was slowly removed and the burr hole and the scalp sutured.

Survival time of the rats was about 2-3 weeks after tumour implantation.

All procedures related to animal care were strictly conformed in accordance with Decree 116/92 which represents the Italian enforcement of the European Directive 86/609/EEC.

Parameter	Protocol: **MSME T2-weighted images**
TR/TE	2500/45 ms
Slice thikness	1.5 mm
Square FOV	40X40 mm
Matrix	128X128 pixels
Resolution	312µmX312 µm

In vivo Imaging results

Axial ^{1}H MR images of rat brain acquired two hours after ^{19}F-BPA-fr complex infusion

Intra-carotid BPA-fr infusion: 300mg/Kg

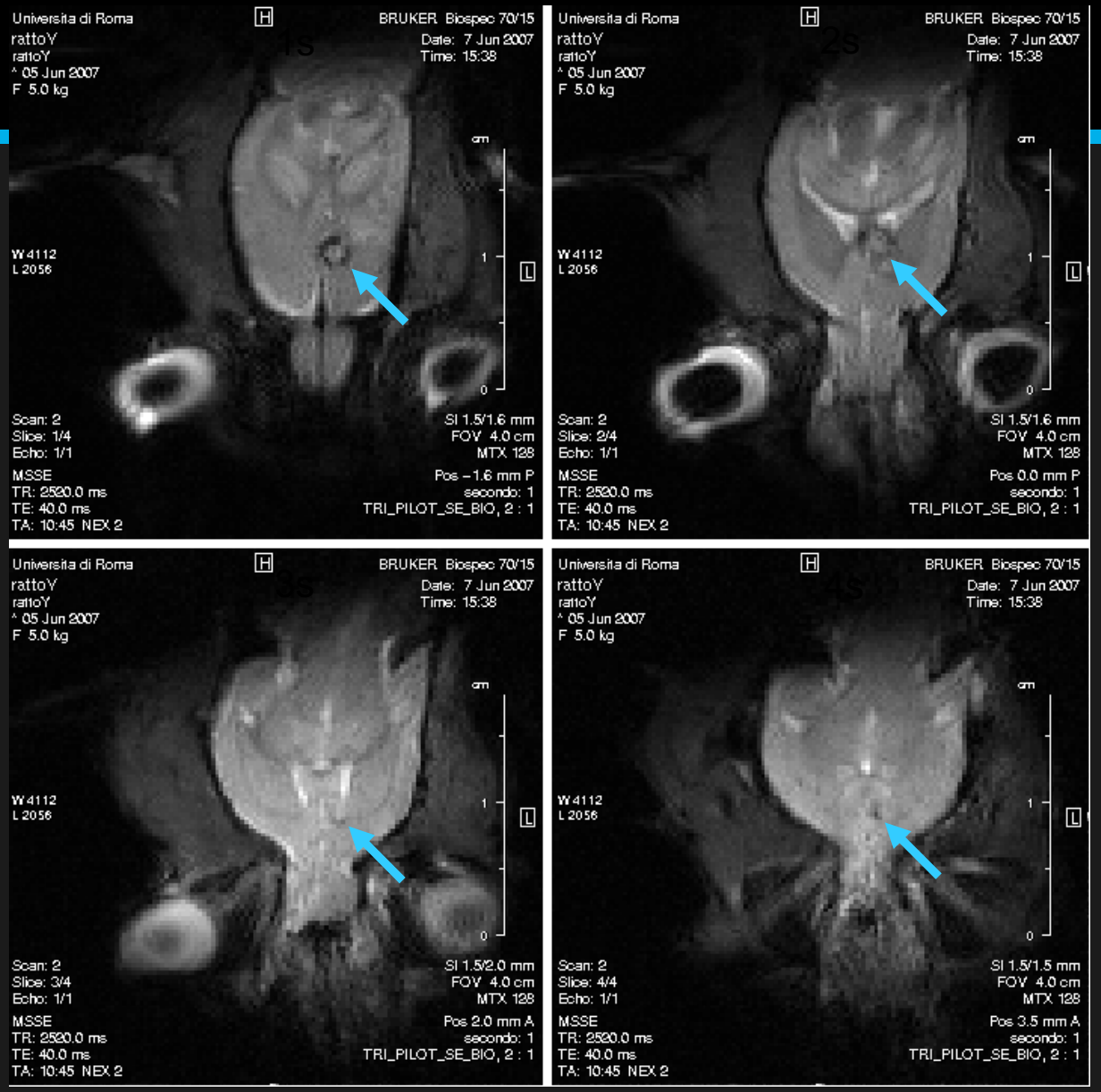

^{19}F axial image of rat brain acquired after ^{1}H MR scan

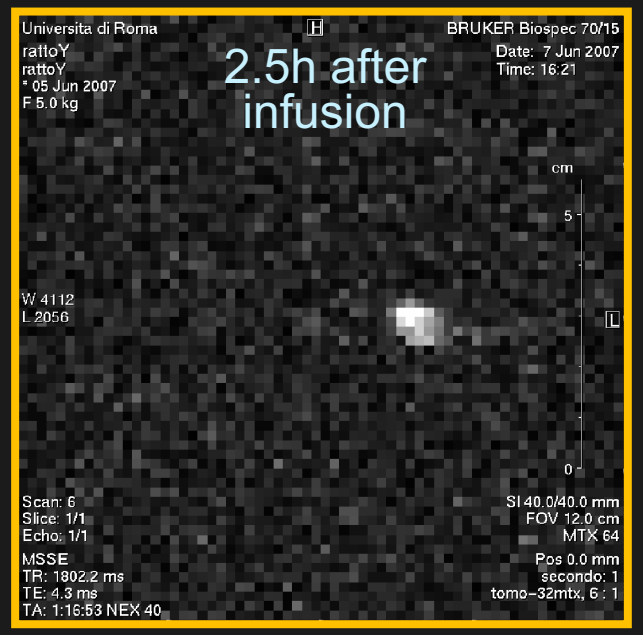

^{19}F-BPA spatial bio-distribution mapping by ^{19}F MRI

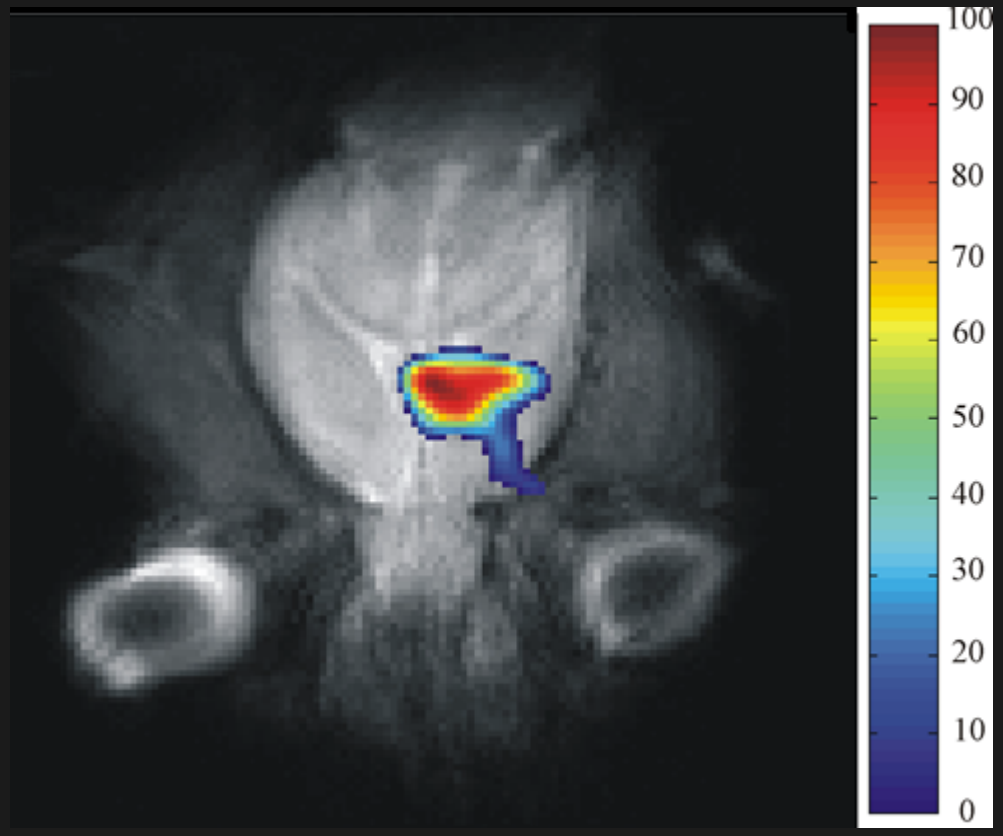

Superimposition of ^{19}F axial image

(in colour level: low=blue, red=high)

acquired 2.5 hours after infusion on the corresponding morphological ^{1}H proton reference (in grey levels).

^{1}H MRI Parameter	Protocol: **MSME T2-weighted images**
TR/TE	2500/45 ms
Slice thikness	1.5 mm
Square FOV	40X40 mm
Matrix	128X128 pixels
Resolution	312μmX312 μm

19F MRI Parameter	Protocol:SE **T2-weighted images**
TR/TE	1800/4.3 ms
Slice thikness	40 mm
Square FOV	120X120 mm
Matrix	64X64 pixels
Resolution	1.85mmX1.85mm
NS	40

P. Porcari, S. Capuani, E. D'Amore *et al.* 2008 *Phys. Med. Biol.*

Pharmacokinetic of ^{19}F-BPA by ^{19}F MRS

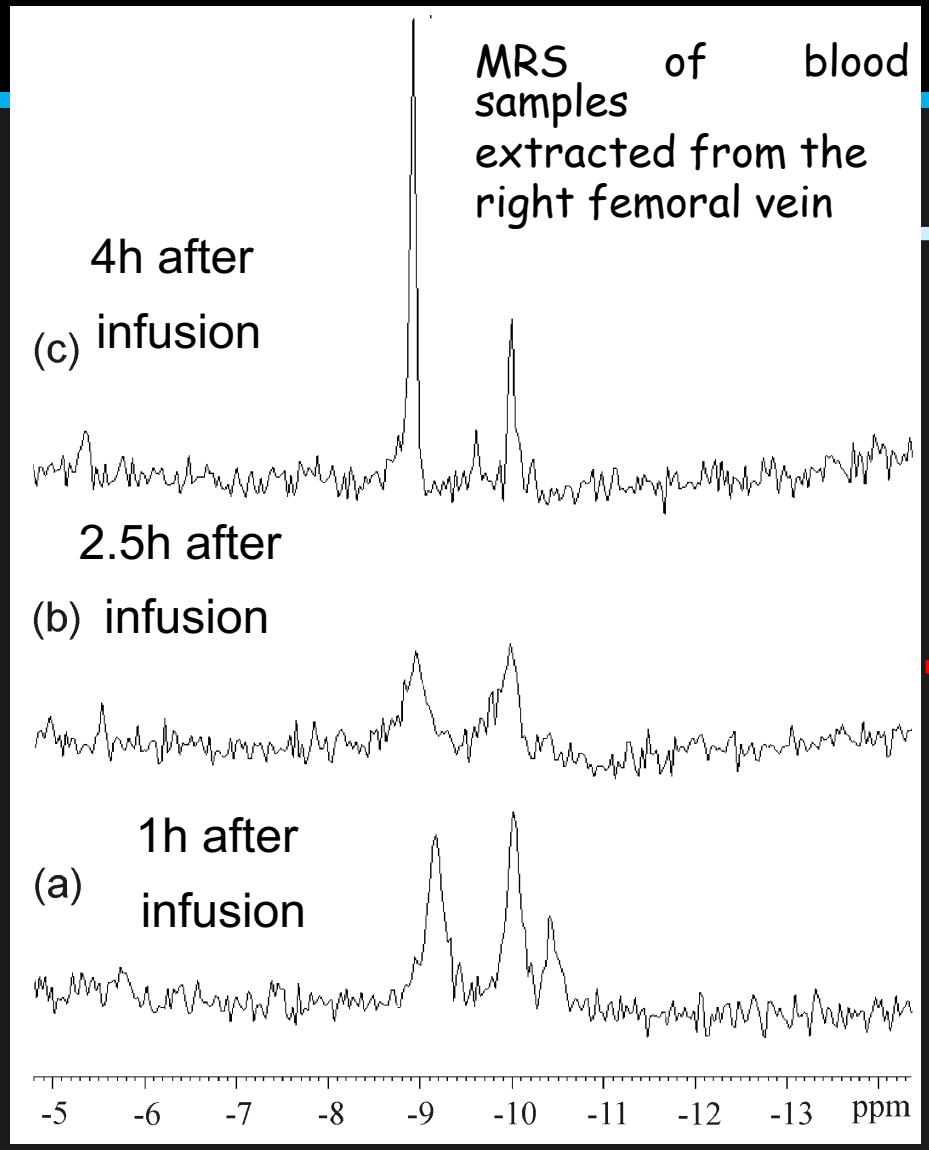

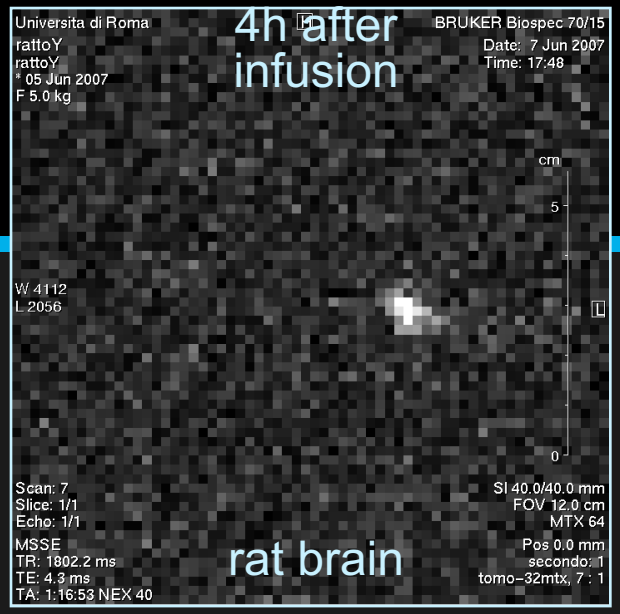

SNR=3.7

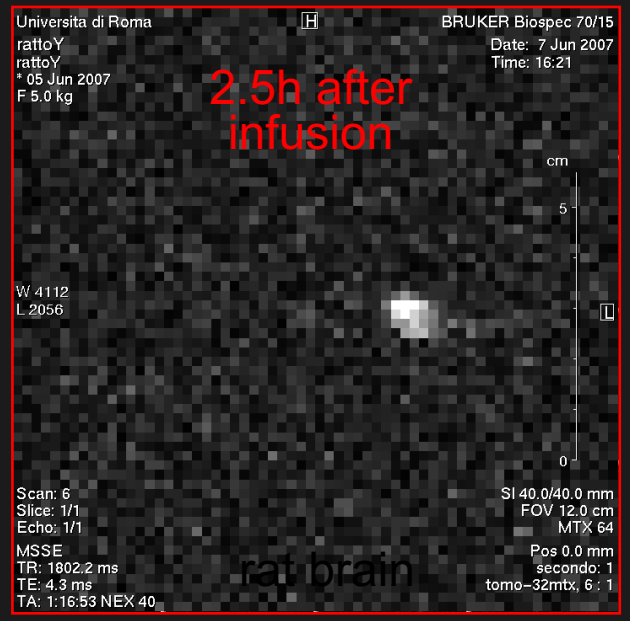

SNR=5.1

2.5 h after infusion the 19F-BPA uptake is maximum in the tumour and minimum in systemic circulation

P. Porcari, S. Capuani, E. D'Amore *et al.* 2008 *Phys. Med. Biol.*

In vivo L-DOPA preloading results

BPA uptake in C6-glioma model is dramatically increased by L-DOPA preloading

Tumor

Normal brain (ipsilateral)

Normal brain (contralateral)

Blood

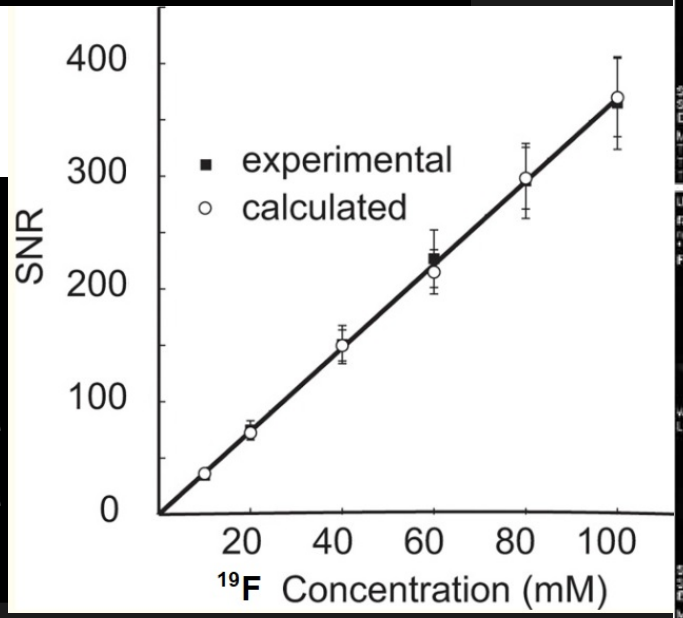

BPA accumulation in tumor samples assessed by HPLC was significantly higher in treated group compared to control group ($p<0.0001$)

S. Capuani, et al. Int J Radiat Oncol Biol Phys 2008

^{1}H ^{19}F

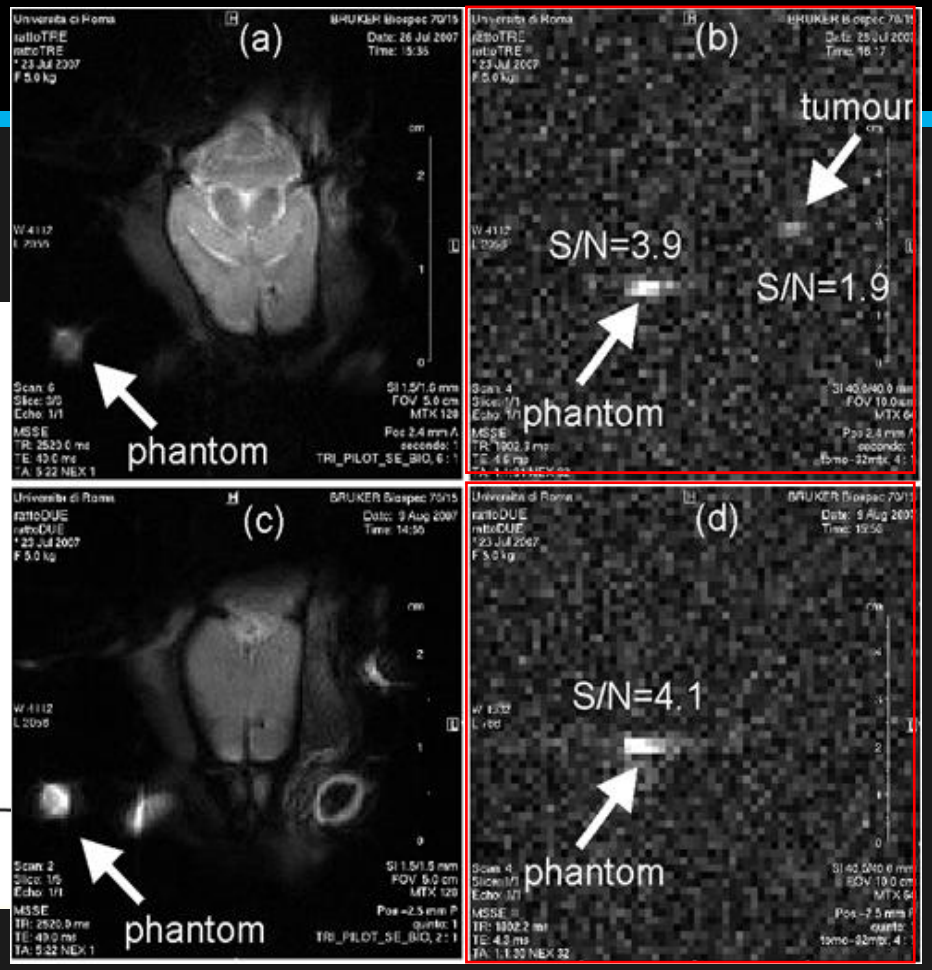

^{19}F-BPA tumour signal was observed only in L-DOPA pre-treated rat but not in the other case confirming an increased ^{19}F-BPA tumour uptake after L-DOPA administration

P. Porcari S. Capuani, E. D'Amore et al. Appl. Rad. Isot. 2009

^{1}H T_2-w image (a) and ^{19}F image (b) of rat brain pre-treated with L-DOPA and then infused with ^{19}F-BPA-fr complex

Phantom:
19F-BPA-frcomplex (10mM) was positioned on the rf coil as a reference during MRI measurements.

^{1}H T_2-w image (c) and ^{19}F image (d) of rat brain not pre-loaded with L-DOPA (control) and then infused with ^{19}F-BPA-fr complex

Conclusion

^{19}F-MRI in combination with ^{1}H-MRI selectively maps the spatial-distribution of ^{19}F-BPA in C6 tumour-bearing rats

- ^{19}F MRI is a useful method to investigate and evaluate the pharmacokinetics of the fluorinated-containing drugs

Correlation between ^{19}F MRI and ^{19}F MRS results highlights an improved understanding of ^{19}F-BPA uptake in tumour and systemic circulation

In order to quantify fluorine-containing molecules in tissues, a phantom containing different drug concentrations should be used in phantom containing pellets or in solutions / gels with similar characteristics to biological tissues

L-DOPA pre-administration produced in the C6 glioma rat model an enhancement of tumor BPA accumulation which was 2.5 times higher than in the control condition

Conclusion and future prospective

In this study we used a drug containing only one 19F

In recent years fluorinated molecules containing many 19F were synthetized to increase image SNR

As an example, using a functionalized perfluorinated emulsion (PFOB)

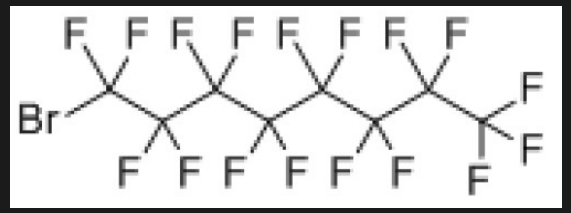

and optimized high sensitivity MSE sequence, Giraudeau et al. (2011) were able to detect about **100 picomolar** concentrations of avβ3-targeted PFOB emulsion in vivo in a U87 human glioblastoma mouse model

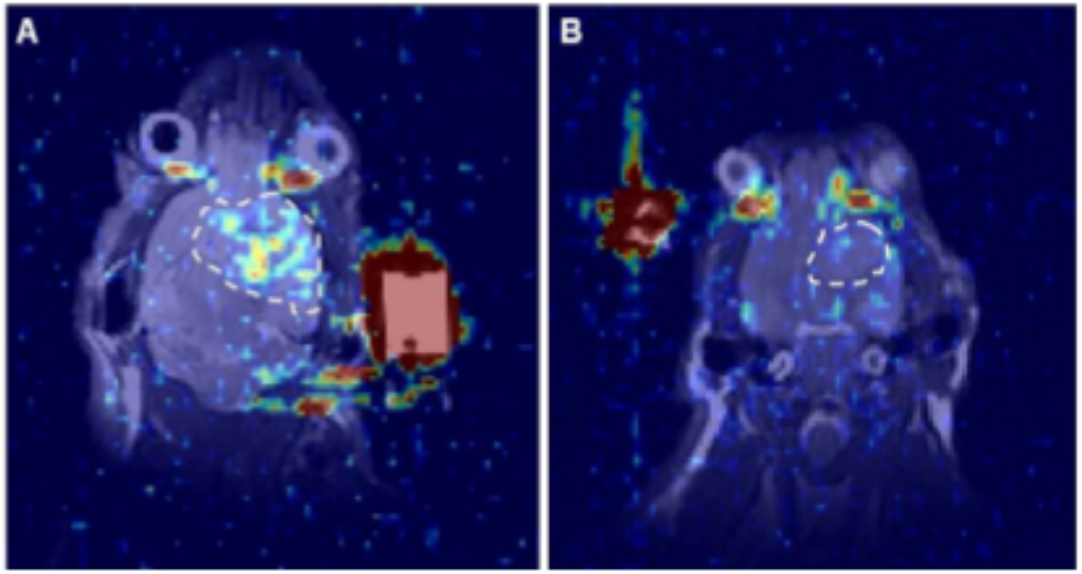

Fig. 1. Superposition of ^{19}F image with anatomical ^{1}H image of mice infused with the targeted (A) and control (B) PFOB emulsions. Tumors are delineated by the white dashed line. ^{19}F signal is clearly visible in the tumor in A, whereas only noise is seen in B. The red spot is the emulsion reference.

Neptune

Tissue: Mouse Pancreas

- Preliminary MRI tests

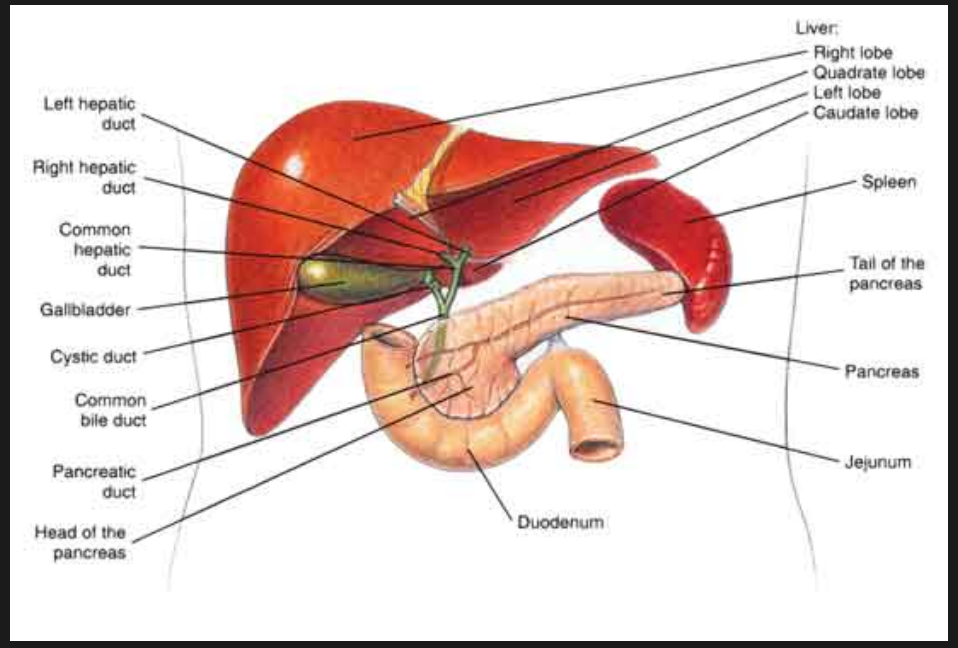

- **Drugs**

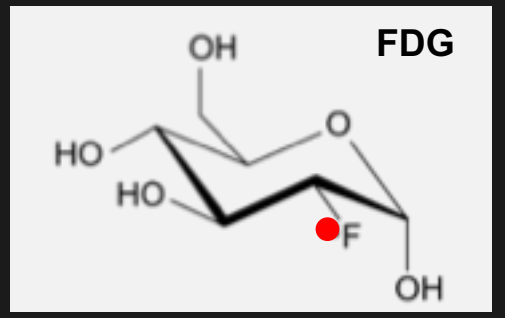

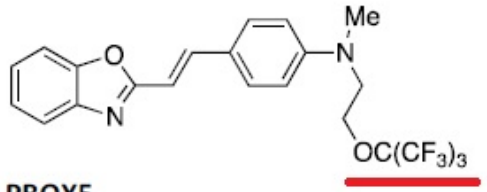

PBOX5

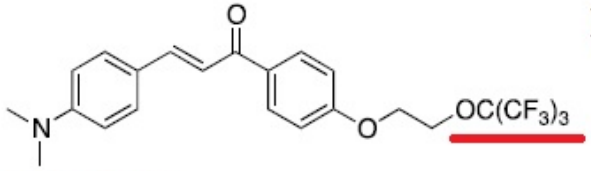

SQ_PRIN_01

Gianluca Pozzi,

CNR-Istituto di Scienze e Tecnologie Molecolari

Milano

Neptune: MRI mouse pancreas features:

Roma, CNR, INFN, ISS

T2w
TE=40ms

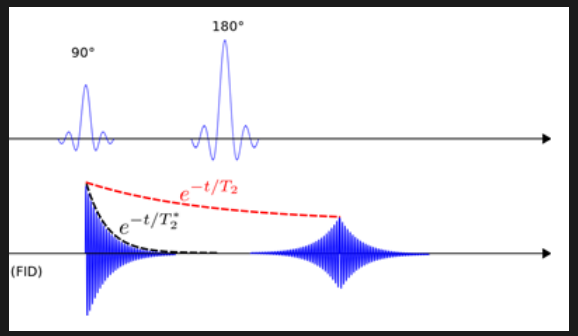

$$S(t) \propto M(T_E) \cong M^0{}_{xy}(1-e^{-\frac{T_R}{T_1}})e^{-\frac{T_E}{T_2}}$$

$$S(b) = S(0)\exp(-bD)$$

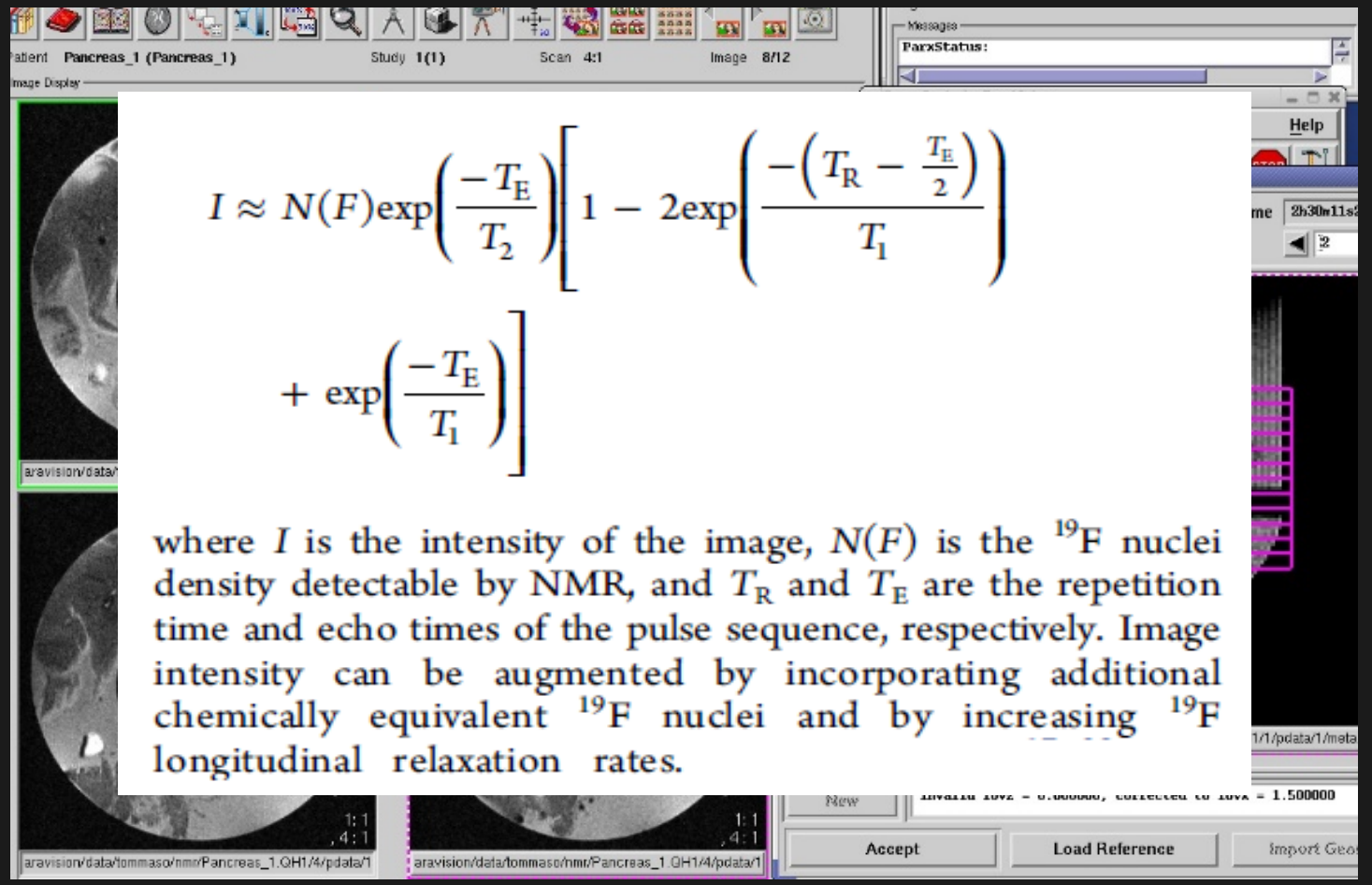

$$I \approx N(F)\exp\left(\frac{-T_E}{T_2}\right)\left[1 - 2\exp\left(\frac{-\left(T_R - \frac{T_E}{2}\right)}{T_1}\right) + \exp\left(\frac{-T_E}{T_1}\right)\right]$$

where I is the intensity of the image, $N(F)$ is the ^{19}F nuclei density detectable by NMR, and T_R and T_E are the repetition time and echo times of the pulse sequence, respectively. Image intensity can be augmented by incorporating additional chemically equivalent ^{19}F nuclei and by increasing ^{19}F longitudinal relaxation rates.

Neptune: MRI mouse pancreas features: relaxation times

Tissue	T2(ms)	T1(ms)
brain	45-80	800
pancreas	22-38	1300

Neptune: MRI mouse pancreas features: diffusion MRI

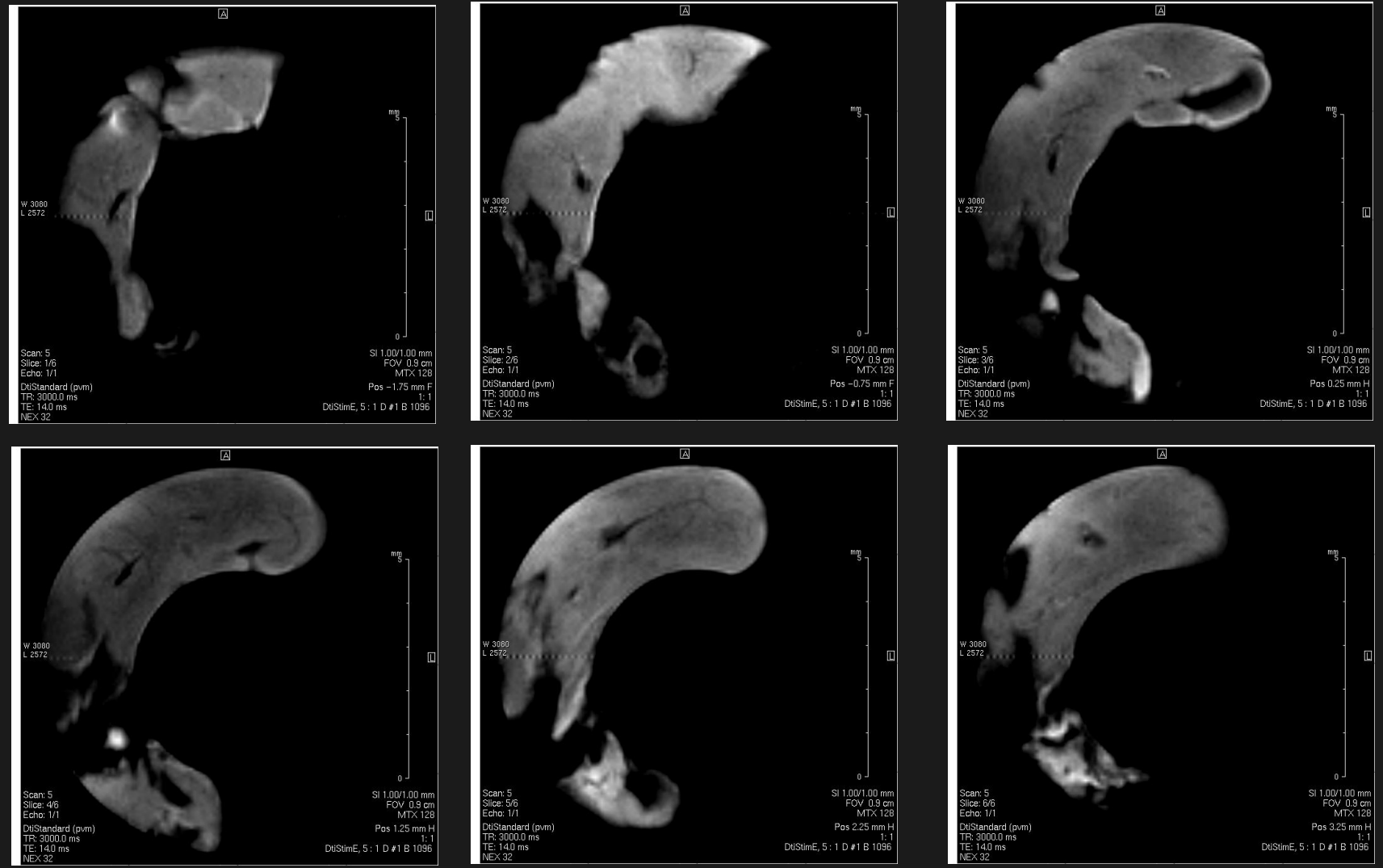

Neptune: MRI mouse pancreas features: diffusion MRI

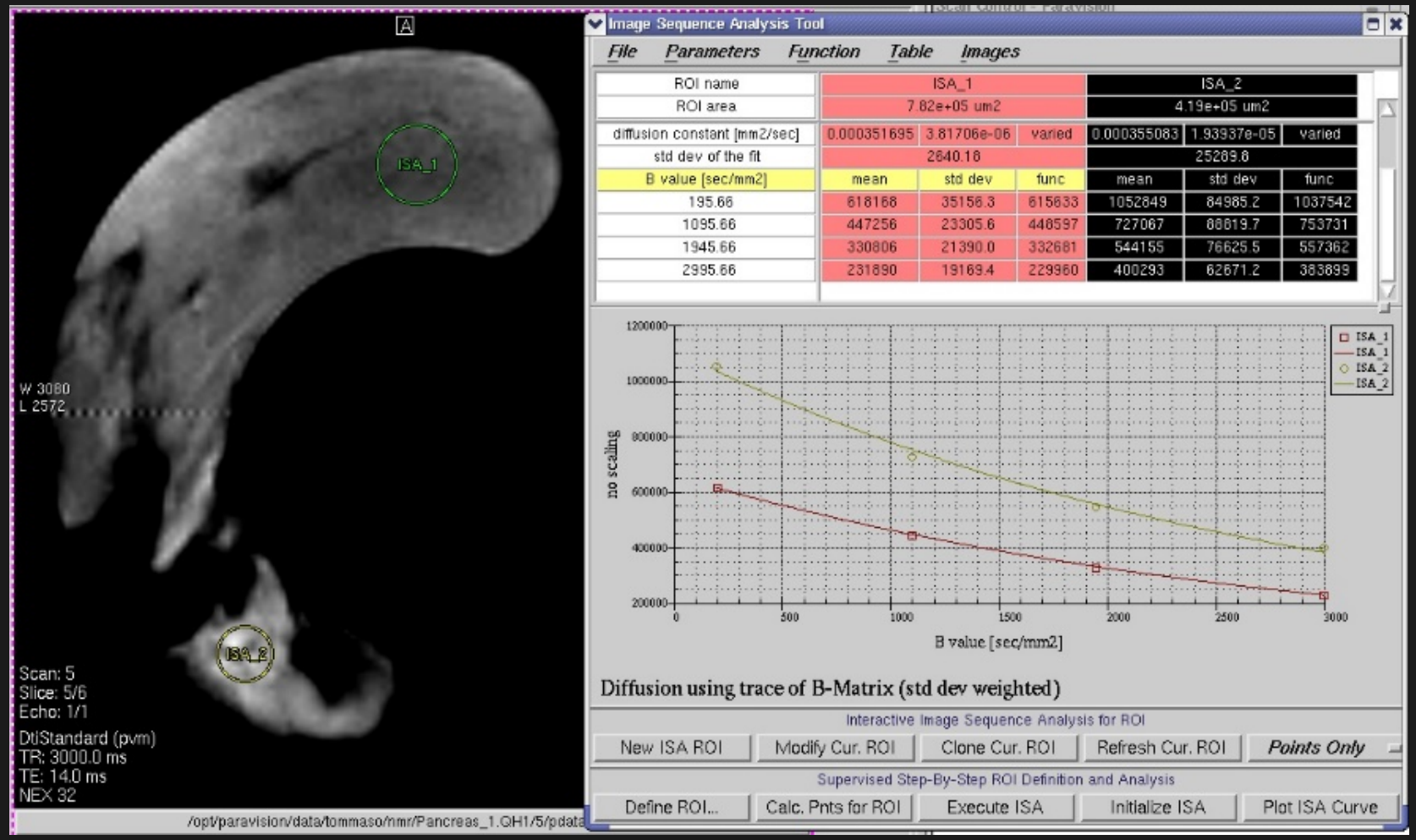

tissue	D(m^2/s)
brain	$9*10^{-10}$
pancreas	$3.5*10^{-10}$

water dynamics slower in the pancreas compared to the cerebral tissue

Neptune: critical aspect, choice of the compound

The pancreatic tissue is more dense than the cerebral one.
Therefore we expect less favorable conditions for the detection of 19F compounds in pancreas compared to brain tissues

With the development of the tumor the tissue becomes denser